Fermi Surface of $Bi_2Sr_2CaCu_2O_8$

H. M. Fretwell,[1,*] A. Kaminski,[1,2] J. Mesot,[2,†] J. C. Campuzano,[1,2] M. R. Norman,[2] M. Randeria,[3] T. Sato,[4] R. Gatt,[1] T. Takahashi,[4] and K. Kadowaki[5]

[1]*Department of Physics, University of Illinois at Chicago, Chicago, Illinois 60607*
[2]*Materials Sciences Division, Argonne National Laboratory, Argonne, Illinois 60439*
[3]*Tata Institute of Fundamental Research, Mumbai 400005, India*
[4]*Department of Physics, Tohoku University, 980-8578 Sendai, Japan*
[5]*Institute of Materials Science, University of Tsukuba, Ibaraki 305, Japan*

(Received 14 October 1999)

We study the Fermi surface of $Bi_2Sr_2CaCu_2O_8$ using angle resolved photoemission spectroscopy (ARPES) with a momentum resolution of ~ 0.01 of the Brillouin zone. We show that, contrary to recent suggestions, the ARPES derived Fermi surface is a large hole barrel centered at (π, π), independent of the incident photon energy. We caution that the photon energy and **k** dependence of the matrix elements, if not properly accounted for, can lead to misinterpretation of ARPES intensities.

PACS numbers: 74.25.Jb, 71.18.+y, 74.72.Hs, 79.60.Bm

The Fermi surface, the locus in momentum space of gapless electronic excitations, is a central concept in the theory of metals. Despite the fact that the optimally doped high temperature superconductors display an anomalous normal state with no well-defined quasiparticles [1], many angle resolved photoemission spectroscopy (ARPES) studies using photon energies in the range of 19–22 eV have consistently revealed a large hole-like Fermi surface centered at (π, π) [2–5] with a volume consistent with the Luttinger count of $(1 - x)$ electrons (where x is the hole doping). This widely accepted picture has recently been challenged by two studies [6,7] which suggest a different ARPES derived Fermi surface when measured at a higher photon energy (32–33 eV). These recent studies propose that the Fermi surface consists of a large *electron* pocket centered on $(0, 0)$ with a clear violation of the Luttinger count. To reconcile their model with previous data at 22 eV photon energy, these authors suggest the presence of "additional states" near $(\pi, 0)$, possibly [7] due to stripe formation. Setting aside for the moment the important question of what the true Fermi surface of $Bi_2Sr_2CaCu_2O_8$ (Bi2212) is, the implication of a photon energy dependent Fermi surface as derived from ARPES data is particularly worrisome, and deserves to be addressed.

Here, we present extensive ARPES data taken at various photon energies and find clear evidence that the Fermi surface as measured by ARPES is independent of photon energy, and consists of a single hole barrel centered at (π, π). Although the data of Refs. [6,7] are consistent with ours, their limited sampling of the Brillouin zone and lower momentum resolution lead to a misinterpretation of the topology of the Fermi surface. This occurs because of the presence of ghost images [5] of the Fermi surface due to diffraction of the outgoing photoelectrons by a Q vector of $\pm(0.21\pi, 0.21\pi)$ associated with the superlattice modulation in the BiO layers (umklapp bands). In particular, in following a Fermi contour, if the data are not dense enough in **k** space, or not of sufficiently high momentum resolution, one can inadvertently "jump" from the main band to one of the umklapp bands, concluding incorrectly that the topology of the Fermi surface is electronlike. This is particularly relevant at the photon energy of 33 eV because of a strong suppression of the ARPES matrix elements at **k** points in the vicinity of $(\pi, 0)$, a final state effect, resulting in a large umklapp/main band signal ratio near $(0.8\pi, 0)$, where the purported electron Fermi surface crossing occurs.

ARPES probes the occupied part of the electron spectrum, and for quasi-2D systems its intensity $I(\mathbf{k}, \omega)$ is proportional to the square of the dipole matrix element, the Fermi function $f(\omega)$, and the one-electron spectral function $A(\mathbf{k}, \omega)$ [8]. The measured energy distribution curve (EDC) is obtained by the convolution of this intensity with experimental resolution. In another paper, we discuss in great detail the various methodologies for determining the Fermi surface from ARPES data [9]. Here, we look at two quantities: (1) the dispersion of spectral peaks obtained from the energy distribution curves, and (2) the ARPES intensity integrated over a narrow energy range about the Fermi energy [4]. As we will show, these methods must be treated with care because of the photon energy and **k** dependence of the matrix elements [9–11], and the presence of the umklapp bands [5].

The ARPES experiments were performed at the Synchrotron Radiation Center, Wisconsin, using a plane grating monochromator beam line with a resolving power of 10^4 at 10^{12} photons/s, combined with a SCIENTA-200 electron analyzer used in an angle resolved mode. A typical measurement involved the simultaneous collection and energy/momentum discrimination of electrons over a $\sim 12°$ range (cut) with an angular resolution window of $\sim(0.5°, 0.26°)$ ($0.26°$ parallel to the cut). This corresponds to a momentum resolution of $(0.038, 0.020)\pi$, $(0.029, 0.015)\pi$, and $(0.022, 0.012)\pi$ at 55, 33, and 22 eV, respectively. The energy resolution for all data was ~ 16 meV (FWHM).

The quality of the optimally doped single crystal samples cannot be emphasized enough, particularly in regards to the flatness of the surface after cleave. A change of 1 μm in height over the width of the sample is readily detectable as a broadening of the spectral features, and therefore care was exercised in studying very flat samples with sharp x-ray diffraction rocking curves. Reference spectra were collected from polycrystalline Au (in electrical contact with the sample) and used to determine the chemical potential (zero binding energy).

To begin we look at data (Fig. 1) taken on an optimally doped Bi2212 sample ($T_c = 90$ K), measured at $T = 40$ K [12] at 33 eV. The light polarization was parallel to ΓX [we use the notation $\Gamma = (0,0)$, $X = (\pi, -\pi)$, $Y = (\pi, \pi)$, and $M = (\pi, 0)$, with ΓY parallel to the superlattice modulation) and EDCs were collected on a regular lattice of **k** points ($\delta k_x = 1°$, $\delta k_y = 0.26°$). We first examine spectra along the ΓY direction. The EDCs are shown in the middle panel of Fig. 1, and the left panel shows a two-dimensional plot of the energy and momentum distribution of the photoelectrons along the ΓY cut. A strong main band (MB) and additional umklapp bands (UB) can be observed in this plot. Around $(0,0)$, there is a weaker pair of higher-order umklapps [UB(2) corresponding to a translation of $\pm(0.42, 0.42)\pi$] as observed previously [13], which confirms the diffraction origin of the umklapp bands. Along this cut, we also see the (π, π) translation of the main band, the so-called shadow band (SB) [4], which is probably [5] associated with the two formula units per base orthorhombic unit cell. Figure 1c shows the integrated intensity within a ± 100 meV window about the chemical potential. We note the very rapid suppression of intensity beyond $\sim 0.8\Gamma M$ [14], which does not occur at 22 eV. This is what led the authors of Refs. [6,7] to suggest the existence of an electronlike Fermi surface with a crossing at this point. As first discussed in an earlier paper which exploited dipole selection rules [5], and addressed in greater detail here, we will demonstrate that instead, this crossing is due to one of the umklapp bands. This umklapp crossing is more obvious at 33 eV, since, unlike at 22 eV, the main band intensity is suppressed. We cannot emphasize enough that this suppression is due to the matrix elements [9,10]. Suggestions [6,7] based on normal state data that the suppression is solely due to the band being above the Fermi energy at M are inconsistent with the fact that the width of the spectral peak is several hundred meV, and thus appreciable signal intensity below the Fermi energy would occur, unlike what is observed. Moreover, as shown in Fig. 1d, our own normal state data (using a smaller integration range) are clearly more consistent with a holelike Fermi surface.

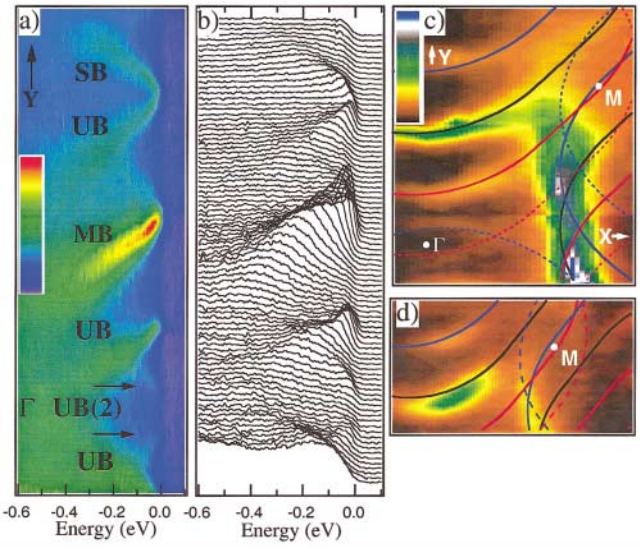

FIG. 1 (color). (a) Intensity $I(\mathbf{k}, \omega)$ and (b) EDCs along ΓY measured on an optimally doped sample ($T_c = 90$ K) at $T = 40$ K with 33 eV photons polarized along ΓX. Main, umklapp, second-order umklapp, and shadow bands are denoted as MB, UB, UB(2), and SB. (c) Integrated intensity (± 100 meV) covering the X and Y quadrants of the Brillouin zone. Data were collected on a regular lattice of **k** points (spacing 1° along ΓX and 0.26° along ΓY). (d) Integrated intensity (± 40 meV) as in (c), but in the normal state ($T = 150$ K). Overlaid on (c) and (d) is the main band (black), $\pm$ umklapps (blue/red), and $\pm$ second-order umklapps (dashed blue/red lines) Fermi surfaces from a tight binding fit [15].

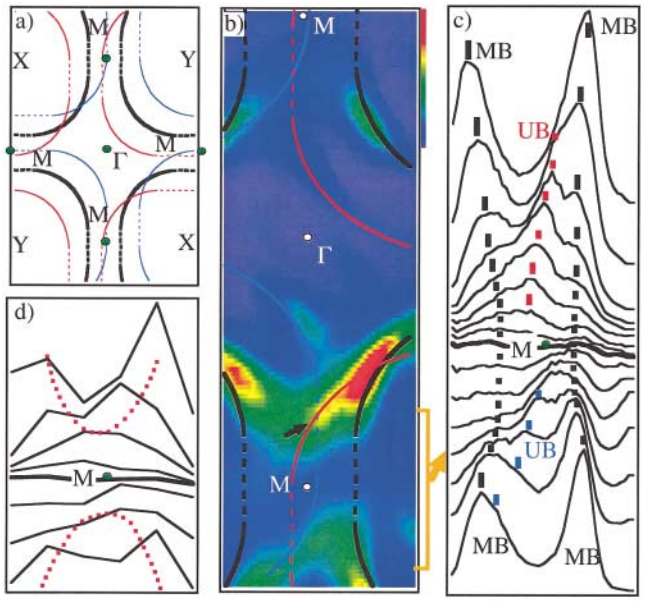

FIG. 2 (color). (a) Tight binding Fermi surface from Ref. [15] and its umklapp images. (b) Integrated intensity (± 100 meV) from four quadrants of the Brillioun zone. Data were measured using 33 eV photons on an optimally doped sample ($T_c = 90$ K) at $T = 40$ K with the same k point spacing as in Fig. 1. Light polarization is along ΓM. Dashed portions on the Fermi surface overlay from (a) indicate intensity suppression due to matrix elements. Note that because of the umklapps, this leads to a diagonal-like suppression of the intensity around M. (c) Slices parallel to MY from (b) in an expanded region about M (thick black line is the MY slice). (d) Data artificially broadened in **k** resolution by interpolating (c) onto a new **k** lattice (spacing 2°). Red dashed lines indicate the Fermi surface contours suggested in Refs. [6,7].

To examine this issue more closely, we measured another optimally doped sample ($T_c = 90$ K, $T = 40$ K) with 33 eV photons polarized parallel to ΓM (shown in Fig. 2) with the same high density of $\mathbf{k}$ points as for the ΓX oriented sample. The integrated intensity at E_F is similar to the ΓX oriented sample in that there is an "apparent" closed Fermi surface around $(0, 0)$, indicated by an arrow in Fig. 2b. However, on closer inspection of the $(\pi, 0)$ region, we see what is truly occurring. Figure 2c shows slices parallel to MY from the plot of Fig. 2b. The MB, indicated by the short black bars, continues to run parallel to ΓM, but its intensity is heavily suppressed near M. In addition, the $(+)$ umklapp band, indicated by red bars, splits away from the main band, disperses towards M, and dies in intensity. A transposed version of this occurs beyond M with the $(-)$ umklapp, indicated in blue. Similar behavior is also seen at the M point at the top of Fig. 2b (slices not shown) and in the ΓX oriented sample of Fig. 1c.

It is easy to see how sparse data at lower resolution can easily lead one to miss the suppressed main band crossing along MY at 33 eV. Figure 2d shows a plot similar to the one in Fig. 2c, but at a resolution of $(0.11, 0.11)\pi$—the same as that used in Ref. [7]—instead of $(0.029, 0.015)\pi$ in Fig. 2c. Clearly, it is no longer possible to distinguish the umklapp from the main band and one might wrongly suppose that the Fermi surface curves around to cross the ΓM line. But we emphasize again that such a supposition is only a result of sparse data, and not of any inherent differences in experimental results. It is worth noting that in the ΓX oriented sample (Fig. 1c) we can see a weak signal corresponding to the main band MY Fermi crossing, which becomes stronger at 22 eV. Therefore, if quantities based on integrated intensity are used to define the Fermi surface, one may falsely infer a crossing along ΓM due to the $(+)$ umklapp band, as indicated in Fig. 2d.

The presence of the umklapps can also explain the origin of the asymmetry in the underlying intensity plot at M in Fig. 2b. At 33 eV the ARPES signal from the main band is strongly suppressed near M due to the matrix elements, but since the umklapps are translated by $\pm(0.21, 0.21)\pi$, we get a diagonal-like suppression of the total signal near M. This can be appreciated by looking at the dashed segments of the overlay on Fig. 2b. That is, the umklapp signal at $\mathbf{k}$ is comparable in intensity to the main band signal at $\mathbf{k} \pm \mathbf{Q}$, as expected if the umklapp is simply a diffraction of the outgoing photoelectrons by the BiO superlattice.

According to this picture, when moving along ΓM, there should be a crossover from the $(+)$ to $(-)$ umklapp, and this is in fact seen in the raw data. Figure 3 shows extensive EDCs taken in cuts parallel to MY at $\mathbf{k}$ points along ΓM for 33 eV. In *most* of these plots, the main band (crossing shown by a black square) is the strongest

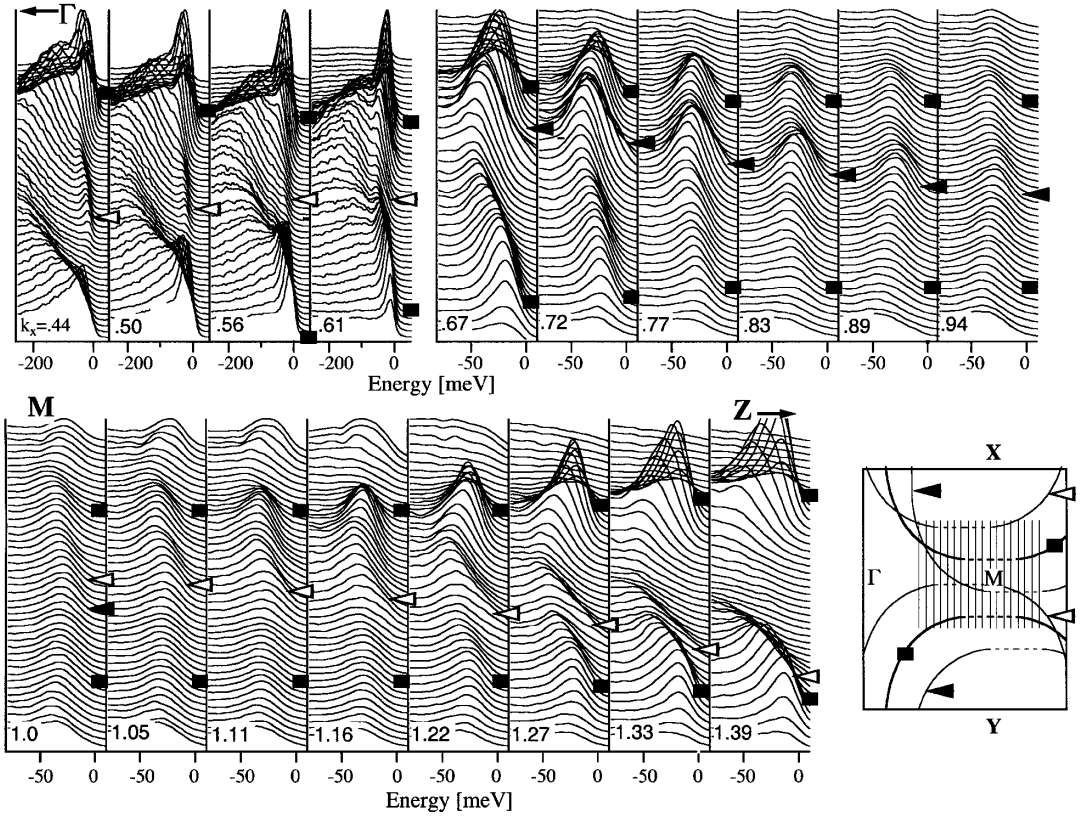

FIG. 3. EDCs for cuts parallel to MY (see inset) measured at $T = 40$ K for 33 eV photon energy. Note change in binding energy axis scale to emphasize quasiparticle dispersion. Same sample and orientation as in Fig. 2. The black squares indicate the main band crossings, and the black and white arrows indicate the umklapp band crossings. The zone inset is as in Fig. 2a, with dashed segments on the Fermi contours indicating matrix element suppression, and the vertical lines representing the cuts.

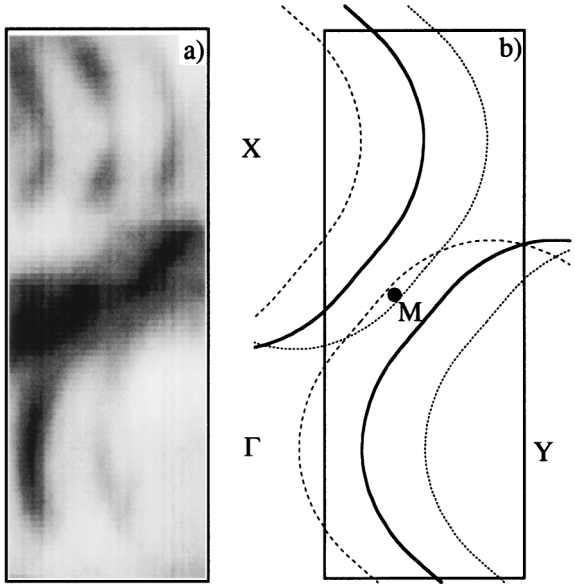

FIG. 4. (a) Near E_F intensity (integrated over ± 100 meV) at 55 eV for the ΓX oriented sample of Fig. 1 measured at $T = 40$ K. Note the striking similarity to the large hole Fermi surface (solid curves) with its umklapp images (dashed curves) shown in (b).

signal and the $\pm$ umklapps (crossings shown as black and white arrows) are a weaker signal superimposed near the ΓM line. A constant offset has been used in the figures so that the umklapp crossings appear as a "bunching" of the spectra. Going from Γ to M we see, in the following order, the $(-)$ umklapp (white arrow), the $(+)$ umklapp (black arrow) which disappears at $(\pi, 0)$, and finally the reappearance of the $(-)$ umklapp (white arrow). We find that the dispersion of all of the main and umklapp signals is consistent with the tight binding fit to the dispersion at 19–22 eV [5,15]. The difference is that, at 22 eV [5], the suppression of the signal at $(\pi, 0)$ is weaker, and the MY crossing of the main band is clearer [9].

In Fig. 4a, we show an intensity map from the sample of Fig. 1, but at 55 eV photon energy. From this intensity plot, one can clearly see the main Fermi surface and its two umklapp images, and the correlation of this image with a single large hole surface around (π, π) together with its predicted umklapp images (Fig. 4b) is striking.

In conclusion, we find that the ARPES derived Fermi surface of Bi2212 is a single hole barrel centered at (π, π), a result which we find to be independent of photon energy. Rather, we have demonstrated that the unusual intensity variation observed by previous authors at 33 eV is caused by a combination of matrix element effects and the presence of umklapp bands caused by the diffraction of the photoelectrons from the BiO superlattice. This emphasizes the need to be cautious when interpreting ARPES intensities.

This work was supported by the U.S. National Science Foundation, Grants No. DMR 9624048 and No. DMR 91-20000 through the NSF Science and Technology Center for Superconductivity, the U.S. Department of Energy Basic Energy Sciences, under Contract No. W-31-109-ENG-38, the CREST of JST, and the Ministry of Education, Science and Culture of Japan. The Synchrotron Radiation Center is supported by the NSF Grant No. DMR-9212658. M. R. was supported in part by the Indian DST through the Swarnajayanti scheme.

*Present address: Dept. of Physics, University of Wales Swansea, Swansea SA2 8PP, United Kingdom.
†Present address: ETH Zurich and Paul Scherrer Institut, CH-5232 Villigen PSI, Switzerland.

[1] A. Kaminski *et al.,* Phys. Rev. Lett. **84**, 1788 (2000).
[2] J. C. Campuzano *et al.,* Phys. Rev. Lett. **64**, 2308 (1990).
[3] C. G. Olson *et al.,* Phys. Rev. B **42**, 381 (1990).
[4] P. Aebi *et al.,* Phys. Rev. Lett. **72**, 2757 (1994).
[5] H. Ding *et al.,* Phys. Rev. Lett. **76**, 1533 (1996).
[6] Y.-D. Chuang *et al.,* Phys. Rev. Lett. **83**, 3717 (1999).
[7] D. L. Feng *et al.,* cond-mat/9908056.
[8] M. Randeria *et al.,* Phys. Rev. Lett. **74**, 4951 (1995).
[9] J. Mesot *et al.,* cond-mat/9910430. In the absence of very dense **k** sampling, one needs to (i) exploit dipole selection rules to separate the main band from umklapp crossings, and to (ii) compare in detail spectra, and their integrated intensity, obtained at different photon energies, to disentangle matrix element effects.
[10] That the strong photon energy dependence is due to matrix elements has been verified by recent theoretical calculations. See A. Bansil and M. Lindroos, Phys. Rev. Lett. **83**, 5154 (1999).
[11] Strong photon energy dependent effects were seen earlier in YBCO. See J. G. Tobin *et al.,* Phys. Rev. B **45**, 5563 (1992).
[12] Despite the fact that the superconducting state is gapped, the presence of sharp quasiparticle peaks facilitates the determination of the underlying Fermi surface, as compared to the normal state, which exhibits broad spectral features [see H. Ding *et al.,* Phys. Rev. Lett. **78**, 2628 (1997)]. We note that the integration range (± 100 meV) employed for the intensity patterns is much larger than the gap energy scale, and that the minimum gap locus in a superconductor is essentially identical to the normal state Fermi surface.
[13] J. Osterwalder *et al.,* Appl. Phys. A **60**, 247 (1995).
[14] N. L. Saini *et al.,* Phys. Rev. Lett. **79**, 3467 (1997).
[15] M. R. Norman *et al.,* Phys. Rev. B **52**, 615 (1995).